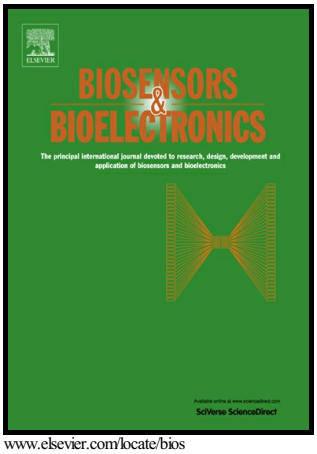

www.elsevier.com/locate/bios

Enzyme-free fluorescent biosensor for the detection of DNA based on CORE-shell Fe_3O_4 polydopamine nanoparticles and hybridization chain reaction amplification

Na Li, Xia Hao, Bei Hua Kang, Zhen Xu, Yan Shi, Nian Bing Li, Hong Qun Luo

PII: S0956-5663(15)30469-3
DOI: http://dx.doi.org/10.1016/j.bios.2015.10.004
Reference: BIOS8040

To appear in: *Biosensors and Bioelectronic*

Received date: 9 July 2015
Revised date: 16 September 2015
Accepted date: 2 October 2015

Cite this article as: Na Li, Xia Hao, Bei Hua Kang, Zhen Xu, Yan Shi, Nian Bin Li and Hong Qun Luo, Enzyme-free fluorescent biosensor for the detection o DNA based on CORE-shell Fe_3O_4 polydopamine nanoparticles and hybridizatio chain reaction amplification, *Biosensors and Bioelectronic* http://dx.doi.org/10.1016/j.bios.2015.10.004

Enzyme-free fluorescent biosensor for the detection of DNA based on core-shell Fe_3O_4 polydopamine nanoparticles and hybridization chain reaction amplification

Na Li, Xia Hao, Bei Hua Kang, Zhen Xu, Yan Shi, Nian Bing Li,* and Hong Qun Luo*

Key Laboratory of Eco-environments in Three Gorges Reservoir Region (Ministry of Education), School of Chemistry and Chemical Engineering, Southwest University, Chongqing 400715, PR China.

*Corresponding Author. Tel: +86 23 68253237; fax: +86 23 68253237; E-mail address: linb@swu.edu.cn (NB Li); luohq@swu.edu.cn (HQ Luo).

Abstract

A novel, highly sensitive assay for quantitative determination of DNA is developed based on hybridization chain reaction (HCR) amplification and the separation via core-shell Fe_3O_4 polydopamine nanoparticles (Fe_3O_4@PDA NPs). In this assay, two hairpin probes are designed, one of which is labeled with a 6-carboxyfluorescein (FAM). Without target DNA, auxiliary hairpin probes are stable in solution. However, when target DNA is present, the HCR between the two hairpins is triggered. The HCR products have sticky ends of 24 nt, which are much longer than the length of sticky ends of auxiliary hairpins (6 nt) and make the adsorption much easier by Fe_3O_4@PDA

NPs. With the addition of Fe_3O_4@PDA NPs, HCR products could be adsorbed because of the strong interaction between their sticky ends and Fe_3O_4@PDA NPs. As a result, supernatant of the solution with target DNA emits weak fluorescence after separation by magnet, which is much lower than that of the blank solution. The detection limit of the proposed method is as low as 0.05 nM. And the sensing method exhibits high selectivity for the determination between perfectly complementary sequence and target with single base-pair mismatch. Importantly, the application of the sensor for DNA detection in human serum shows that the proposed method works well for biological samples.

Keywords: enzyme free; DNA; Fe_3O_4 polydopamine nanoparticles; hybridization chain reaction

1. Introduction

The sensitive and selective detection of nucleic acids is of great significance in early diagnosis of disease, mutation detection, and biodefence applications (Cao et al., 2002; He et al., 2010; Ho et al., 2002; Nam et al., 2004). Moreover, it is important to develop the approaches that can detect trace specific sequences because the DNA sequences of interest are usually present in very small amounts. In recent years, DNA amplification techniques have attracted substantial research interest, such as polymerase chain reaction (PCR) (Heim et al., 2003; Chan et al., 2014), ligase chain reaction (LCR) (Zhu et al., 2014; Song et al., 2013), and some isothermal amplification techniques (Lin et al., 2006; Murakami et al., 2009; Xuan et al., 2012;

Fan et al., 2012; Zhuang et al., 2014). However, these methods highly depend on the activity of enzymes. Thus, enzyme-assisted amplifications require precisely controlled reaction conditions, such as temperature, pH, and buffer media. In addition, as environmental media are vital to guarantee the enzyme activity, relatively clean samples are needed during DNA detection, making it difficult to detect target DNA in complicated biological samples.

Hybridization chain reaction (HCR), as a kind of enzyme-free amplification method (Ge et al., 2014; Huang et al., 2011; Liu et al., 2013; Xuan et al., 2014), was introduced by Dirks and Pierce (Dirks et al., 2004). In HCR, two kinds of hairpin probes are rationally designed and can coexist stably in solution before the introduction of initiator strand. The initiator triggers a cascade of hybridization events between the two metastable hairpin probes. As a result, long-nicked double helices are yielded which are analogous to alternating copolymers.

Nanomaterials have attracted immense scientific and technological attention because of their unique electronic, optical, and catalytic properties (Lou et al., 2015; Tan et al., 2011; Xie et al., 2014). And some of them have been exploited for developing biosensors because of the tight binding with single-stranded DNA (ssDNA), such as graphene oxide (GO) (He et al., 2010), gold nanoparticles (AuNPs) (Tan et al., 2011), MoS_2 nanosheets (Zhu et al., 2013), carbon nanoparticles (Lin et al., 2014), and carbon nanotubes (Wu et al., 2008). However, the preparations of these nanomaterials are usually fussy and elaborate, and some nanomaterials are found to be toxic for in vivo studies, which greatly limits their applications. Bioinspired

polydopamine nanoparticles as a kind of nanomaterials with excellent biocompatibility and biodegradability were reported in 2014 (Qiang et al., 2014). In the report, single-stranded DNA could be adsorbed on polydopamine nanoparticles by π-π stacking, which led to the quenching of fluorescence. Besides, uniform core-shell nanoparticles are of scientific interest because of their magnetically responsive cores and functional shells (Gao et al., 2007; Lu et al., 2013; Polshettiwar et al., 2011; Stoeva et al., 2005). Polydopamine can coat on the core of Fe_3O_4 by dopamine self-polymerizing at alkaline pH values, which enables the formation of core-shell Fe_3O_4 polydopamine nanoparticles (Fe_3O_4@PDA NPs) (Lee et al., 2007). Most of the reports were focused on the synthesis of nanoparticles by using the coating property of PDA. However, the fabrication of fluorescent sensor for target DNA detection using Fe_3O_4@PDA NPs as a separation material has not been reported.

Herein, we utilize decreased signal for DNA detection by combining the signal amplification by HCR and separation using Fe_3O_4@PDA NPs via π-π stacking. Two specially designed hairpin probes are employed in the assay. When target DNA is present in the solution, it initiates the reaction of hybridization chain. And each HCR product has a longer sticky end (24 nt) than that of hairpin (6 nt). Fe_3O_4@PDA NPs are an attractive nanomaterial with excellent biocompatibility. More importantly, it has distinct adsorption properties for ssDNA and the interaction becomes stronger when the ssDNA is longer. When Fe_3O_4@PDA NPs are introduced to HCR products, decreased fluorescence signal is observed in supernatant after the separation. As a result, the fluorescence intensity decreases with increasing concentration of target

DNA. The enzyme-free, fluorescent sensor with high sensitivity and selectivity is capable of functioning in complex samples, such as blood serum, revealing highly practical applicability.

2. Materials and methods

2.1. Materials and reagents

Lyophilized oligonucleotide sequences designed in this study were synthesized and labeled by Sangon Biotech Co., Ltd., Shanghai, China. The sequences of all oligonucleotides are listed in Table S1. The Fe_3O_4 nanoparticles, 2-amino-2-(hydroxymethyl)-1,3-propanediol (tris), and dopamine were purchased from Aladdin Chemistry Co., Ltd. (Shanghai, China) and used as received. All other reagents and chemicals of analytical reagent grade were purchased from Chengdu Kelong Chemical Reagents Factory (China) and used without further purification. Two kinds of buffers were involved in this study: 10 mM Tris-HCl buffer (pH 8.5) and 5 mM Tris-HCl buffer (50 mM $MgCl_2$, pH 8.0). Ultrapure water (specific resistance of 18.2 MΩ cm) was used in each experiment.

2.2. Apparatus

Fluorescence spectra and intensities were measured on a Hitachi F-4500 spectrofluorophotometer (Tokyo, Japan) with the equipment of a 150 W xenon lamp. The slits (Ex/Em) were set at 10.0/10.0 nm and the photomultiplier voltage was 400 V in this assay. To obtain the fluorescence emission spectra, the samples were excited at 490 nm and the emission wavelengths covered the range from 510 to 630 nm. A

scanning electron microscopy (SEM) image was taken on the scanning electron microscopy (JEOL-7800F, Japan). The morphologies of nanoparticles were analyzed on a Philips (FEI) Tecnai G2 F20 transmission electron microscope (TEM) operated at 200 kV. The Fourier transform infrared (FT-IR) spectra were measured by using a Bruker IFS (Germany) 113v spectrometer after pelleting the fine powder with KBr. The SD-101-005DB super digital thermostat bath (Sida Experimental Equipment Ltd., Chongqing, China) was used to keep temperature of the assay. A rapid mixing device (Ronghua Instrument Plant, Jiangsu, China) was used for mixing solutions completely. A pHS-3C pH meter (Shanghai Analytical Instrument Factory, Shanghai, China) was used for adjusting pH values.

2.3. Preparation of Fe_3O_4@PDA NPs

Magnetic Fe_3O_4 polydopamine nanoparticles were prepared according to a previous report (Xie et al., 2014). In order to coat polydopamine shell on the Fe_3O_4 nanoparticles, 80 mg of dopamine and 80 mg of Fe_3O_4 were dispersed in 40 mL of Tris-HCl buffer (10 mM, pH 8.5) and reacted for 24 h under stirring at room temperature. Thereafter, the resulting product was separated with a magnet and washed with ultrapure water and ethanol for several times. And the synthetized Fe_3O_4@PDA NPs were stored in a refrigerator at 4 ^oC before use.

2.4. Measurement procedure for target DNA detection

In a typical detection of target DNA assay, hairpin DNA probes (H1 and H2) were separately heated at 90 ^oC for 2 min and cooled down to room temperature before use.

In a final volume of 500 μL reaction solution, different concentrations of target DNA were incubated with 100 nM H1 and 100 nM H2 in 5 mM Tris-HCl buffer (50 mM $MgCl_2$, pH 8.0) for 4 h at 25 ^oC. Thereafter, previously prepared Fe_3O_4@PDA NPs (1.8 mg mL^{-1}) were added to the solution and the final mixture was incubated for 10 min, followed by a separation using ferromagnet. At last, the fluorescence signals of supernatants were recorded on a spectrofluorophotometer.

3. Results and discussion

3.1. Characterization of Fe_3O_4@PDA NPs

The morphology of Fe_3O_4@PDA NPs was characterized by SEM and TEM. Fig. 1 exhibits the images of Fe_3O_4@PDA NPs prepared by adding Fe_3O_4 nanoparticles to the Tris-HCl buffer containing dopamine. As illustrated in Fig. 1A, uniform Fe_3O_4@PDA NPs were successfully synthesized with a distinct core-shell structure. And the thin polydopamine shell layers formed around the Fe_3O_4 cores present an average thickness of about 20 nm (Fig. 1B). Besides, Fourier transform infrared spectroscopy (FTIR) was used to qualitatively determine adsorption of polydopamine on the surface of Fe_3O_4 nanoparticles. Fig. S1 presents the FTIR spectra of the Fe_3O_4@PDA NPs and Fe_3O_4 nanoparticles. The characteristic bands at 3422, 3051, 2972, 2930, 1630, and 1506 cm^{-1} could only be distinguished in the spectrum of Fe_3O_4@PDA NPs. Compared with the standard spectra, the absorption band at 3422 cm^{-1} indicated the vibration of N-H and O-H bonds. Characteristic bands at 1630 and 1506 cm^{-1} could be attributed to the vibration of C=C in the benzene ring. And the

bands at 3051, 2972, and 2930 cm^{-1} perhaps represented the vibration of C-H bond. All of these bands showed that polydopamine was successfully coated on the surface of Fe_3O_4 nanoparticles.

(Here Fig. 1)

3.2. Design strategy

In this work, the biosensor combined with HCR for signal amplification and Fe_3O_4@PDA NPs for separation is first introduced into the detection of target DNA. The schematic diagram in Scheme 1 illustrates the principle of developed biosensor for target DNA detection. In this assay, two auxiliary hairpin DNA with sticky ends (H1 and FAM-labeled H2) were designed. H1 and H2 both consist of two fragments. Fragment a at 5′ end of H1 can hybridize with fragment a′ of H2. And fragment b at 3′ end of H1 is complementary to fragment b′ of H2. Besides, target DNA can hybridize with fragment a at the 5′ end of H1. In the absence of target DNA, the designed hairpin probes coexist stably in solution with an extra sticky tail of 6 nt. However, upon addition of the target DNA to the solution, it pairs with the sticky end of H1. And the hairpin is unfolded because of an unbiased strand-displacement interaction. Subsequently, the exposed sticky end of H1, fragment b, hybridizes with the sticky end of H2 to open the H2 hairpin and exposes a sticky end, fregment a′. And the sequence of this sticky end is exactly the same with that of target DNA. In this manner, each target DNA can trigger a hybridization chain reaction between alternating H1 and H2 hairpin probes. In addition, each HCR product is a nicked

double-stranded DNA (dsDNA) with 24 nt exposed sticky end. After the separation by using Fe_3O_4@PDA NPs, the fluorescence of the supernatant is decreased, which is different from the system with graphene oxide (GO) and HCR (Yang et al., 2012). The difference might be attributed to the fact that the GO/HCR system has no the procedure of separation, even though the HCR products are dominantly located on the GO surface rather than in the solution. In this assay, the decreased signal obtained with addition of target DNA might be attributed to the following reasons. Firstly, the length of the exposed sticky end of HCR product, 24 nt, is much longer than that of hairpins (6 nt), which means stronger affinity with Fe_3O_4@PDA NPs. Secondly, the number of DNA with sticky ends is greatly decreased after HCR compared with that of hairpins in blank solution, which perhaps saves the bonding sites for Fe_3O_4@PDA NPs. A novel target DNA sensing method was successfully developed based on the change of fluorescence signal caused by the target.

(Here Scheme 1)

3.3. Feasibility tests for the assay

To confirm the feasibility of the design, the fluorescence emission spectra of three different phases of the experiment were recorded. As shown in Fig. 2A, the solution containing H1 and H2 emitted strong fluorescence (curve a). After the introduction of Fe_3O_4@PDA NPs into the solution, the fluorescence signal of supernatant decreased by about 33% after separation (curve b). Interestingly, when target DNA was present, the fluorescence signal of supernatant was reduced greatly (curve c). As a result,

target DNA triggered the hybridization chain reaction upon the addition of target DNA to the solution. And each HCR product has a sticky end of 24 nt, which is much longer than that of hairpins (6 nt), resulting in homogeneous and rapid capture of HCR products by Fe_3O_4@PDA NPs. The interaction between Fe_3O_4@PDA NPs and hairpins with different lengths of sticky ends (HP0, HP6, HP12, and HP18) was investigated. As shown in Fig. 2B, hairpins with longer sticky ends present stronger interation with Fe_3O_4@PDA NPs at various concentrations. Thus, the HCR products can be strongly adsorbed by Fe_3O_4@PDA NPs through π-π stacking, resulting in low fluorescence signal in supernatant after separation.

(Here Fig. 2)

3.4. Optimization of assay conditions

As the performance of Fe_3O_4@PDA NPs played an important role in the proposed method, the fluorescence signal decrease percentage ($1-F/F_0$) against different concentrations of Fe_3O_4@PDA NPs was explored, where F and F_0 were the fluorescence intensities at 522 nm at the excitation wavelength of 490 nm gained in the presence and absence of target DNA, respectively. As shown in Fig. S2, the signal decrease percentage increased and then reached a plateau when the concentration of Fe_3O_4@PDA NPs was higher than 1.8 mg mL^{-1}. And a higher fluorescence signal decrease percentage was more favorable to obtain highly sensitive detection. Thus, 1.8 mg mL^{-1} Fe_3O_4@PDA NPs was chosen as the optimum concentration in the following experiments.

The effect of reaction time on the HCR system was also studied and optimized (Fig. S3). The signal decrease percentage increased sharply at the beginning of HCR. When the HCR carried out for more than 4 h, the signal decrease percentage almost kept stable and did not increase any more. Therefore, 4 h was selected as the optimum reaction time for further analytical detection. Some other assay conditions, such as reaction temperature for HCR, pH, and ionic strength were optimized (Figs. S4-S6). On the basis of these results, an enzyme-free fluorescent biosensor at room temperature in a pH 8.0 Tris-HCl buffer containing 50 mM $MgCl_2$ was selected for the following experiments.

3.5. Fluorescence detection of the target DNA

The sensitivity of the purposed method was evaluated by changing the concentration of target DNA. Under optimum conditions, the fluorescence corresponding to different concentrations of target DNA were detected and analyzed. The fluorescence spectra of the system upon the addition of target DNA are shown in Fig. 3. In the absence of target DNA, the solution emitted strong fluorescence. It was also found that the fluorescence intensity (FL) at 522 nm was highly sensitive to the target DNA and decreased with increasing concentration of target DNA. The dependence of fluorescence intensity on target DNA concentration is plotted in Fig. 3, inset. And the fluorescence intensity was proportional to the concentration of target DNA in the dynamic range of 0 to 1 nM. The regression equation is expressed as $y = -141.38x + 482.06$, with a correlation coefficient R of 0.9914, where y is the fluorescence intensity and x is the concentration of target DNA. The detection limit,

based on 3σ/slope (where σ was the standard deviation of the background signal, n = 11), was calculated to be 0.05 nM, which was comparable with those in literature using polydopamine nanoparticles for DNA detection (Liu et al., 2014; Qiang et al., 2014; Qiang et al., 2015; Xie et al., 2015).

(Here Fig. 3)

3.6. Selectivity of target detection

The selectivity of the detection method was also examined by monitoring the decrease in the percentage of fluorescence signal when the sensing system was challenged with four kinds of DNA sequences, including the perfectly complementary sequence (T), one base-mismatched sequence (M1), one base-deleted sequence (D1), and three base-mismatched sequence (M3). As depicted in Fig. 4, T produced a significantly higher signal decrease percentage ($1-F/F_0$) compared to those caused by other three sequences even though they were of same concentration. When there were three bases mismatched in target DNA, little decrease in fluorescence was observed. And the fluorescence signal decrease percentage of M1 and D1 increased slightly compared to that of M3. Moreover, it is noted that the single base-mismatched target led to a much lower fluorescence signal decrease percentage compared to that of perfectly complementary sequence. In addition, the selectivity of fluorescent sensor was further investigated when the concentration of mismatched DNA was double that of target DNA (Fig. S7). It was found that target DNA triggered an obviously higher signal decrease percentage compared to those caused by other three sequences. To

some extent, the assay can discriminate one-base difference among the DNA targets, indicating high specificity for the target.

(Here Fig. 4)

3.7. Analytical application to complex matrix

To evaluate whether the sensing system could be applied to the determination of target DNA in biological samples, the human serum was employed as complex matrix. Recovery experiments for complex sample matrix, 1 % human serum, were carried out. Then, the human serum samples were spiked with the target DNA at different concentrations (0.3, 0.5, and 1.0 nM). As shown in Fig. S8, the decrease percentage of fluorescence signals ($1-F/F_0$) acquired from the serum samples was consistent with that from Tris-HCl buffer. And the corresponding recoveries were calculated to be 93.72 ± 2.6 %, 101.48 ± 3.7 %, and 90.06 ± 2.8 % for 0.3, 0.5, and 1.0 nM target DNA, respectively. It was found that the proposed method had great potential for the determination of target DNA in real biological samples.

4. Conclusions

An enzyme-free, sensitive, and selective sensing method has been developed for the detection of target DNA combining HCR and Fe_3O_4@PDA NPs. In the proposed method, target DNA triggered the formation of duplex chains with long sticky ends. The HCR amplification guaranteed high sensitivity of the system. Fe_3O_4@PDA NPs functioned as a novel signal controller because the interaction between Fe_3O_4@PDA

NPs and DNA with different lengths of sticky ends was different. The detection limit of the sensing system was experimentally obtained as 0.05 nM. More interestingly, we firstly utilize decreased signal for DNA detection by integration HCR and separation using Fe_3O_4@PDA NPs via π-π stacking, which holds promising potential to broaden the sensing approaches for biomolecule detection, environmental monitoring, and so on.

Acknowledgment

This work was financially supported by the National Natural Science Foundation of China (No. 21273174) and the Municipal Natural Science Foundation of Chongqing City (No. CSTC–2013jjB00002).

Appendix A. Supplementary material

Supplementary material associated with this article can be found in the online version at doi:10.1016/j.bios.201X.XX.XXX.

References

Cao, Y.C., Jin, R., Mirkin, C.A., 2002. Science 297, 1536-1540.

Chan, W.S., Tang, B.S.F., Boost, M.V., Chow, C., Leung, P.H.M., 2014. Biosens. Bioelectron. 53, 105-111.

Dirks, R.M., Pierce, N.A., 2004. Proc. Natl. Acad. Sci. USA 101, 15275-15278.

Fan, Q., Zhao, J., Li, H., Zhu, L., Li, G.X., 2012. Biosens. Bioelectron. 33, 211-215.

Ge, J., Huang, Z.M., Xi, Q., Yu, R.Q., Jiang, J.H., Chu, X., 2014. Chem. Commun. 50,

11879-11882.

Gao, J., Liang, G., Zhang, B., Kuang, Y., Zhang, X., Xu, B., 2007. J. Am. Chem. Soc. 129, 1428-1433.

Heim, A., Ebnet, C., Harste, G., Pring-Akerblom, P., 2003. J. Med. Virol. 70, 228-239.

He, S., Song, B., Li, D., Zhu, C., Qi, W., Wen, Y., Wang, L., Song, S., Fang, H., Fan, C., 2010. Adv. Funct. Mater. 20, 453-459.

Ho, H.A., Boissinot, M., Bergeron, M.G., Corbeil, G., Doré , K., Boudreau, D., Leclerc, M., 2002. Angew. Chem., Int. Ed. 114, 1618-1621.

Huang, J., Wu, Y., Chen, Y., Zhu, Z., Yang, X., Yang, C.J., Wang, K., Tan, W., 2011. Angew. Chem., Int. Ed. 50, 401-404.

Lee, H., Dellatore, S.M., Miller, W.M., Messersmith, P.B., 2007. Science 318, 426-430.

Lin, C., Xie, M., Chen, J.J., Liu, Y., Yan, H., 2006. Angew. Chem., Int. Ed. 45, 7537-7539.

Lin, X., Cui, L., Huang, Y., Lin, Y., Xie, Y., Zhu, Z., Yin, B., Chen, X., Yang, C.J., 2014. Chem. Commun. 50, 7646-7648.

Liu, P., Yang, X., Sun, S., Wang, Q., Wang, K., Huang, J., Liu, J., He, L., 2013. Anal. Chem. 85, 7689-7695.

Liu, Q., Pu, Z.H., Asiri, A.M., Al-Youbi, A.O., Sun, X.P., 2014. Sens. Actuators, B 191, 567-571.

Lou, J., Liu, S., Tu, W., Dai, Z., 2015. Anal. Chem. 87, 1145-1151.

Lu, J., Paulsen, I.T., Jin, D., 2013. Anal. Chem. 85, 8240-8245.

Murakami, T., Sumaoka, J., Komiyama, M., 2009. Nucleic Acids Res. 37 (e19), 1-9.

Nam, J.M., Stoeva, S.I., Mirkin, C.A., 2004. J. Am. Chem. Soc. 126, 5932-5933.

Polshettiwar, V., Luque, R., Fihri, A., Zhu, H., Bouhrara, M., Bassett, J. M., 2011. Chem. Rev.

111, 3036-3075.

Qiang, W., Li, W., Li, X., Chen, X., Xu, D., 2014. Chem. Sci. 5, 3018-3024.

Qiang, W.B., Wang, X., Li, W., Chen, X., Li, H., Xu, D.K., 2015. Biosens. Bioelectron. 71, 143-149.

Stoeva, S.I., Huo, F.W., Lee, J.S., Mirkin, C.A., 2005. J. Am. Chem. Soc. 127, 15362-15363.

Song, Y., Zhang, Y., Wang, T.H., 2013. Small 9, 1096-1105.

Tan, Y.N., Lee, K.H., Su, X., 2011. Anal. Chem. 83, 4251-4257.

Wu, Y., Phillips, J.A., Liu, H., Yang, R., Tan, W., 2008. ACS Nano 2, 2023-2028.

Xie, Y., Yan, B., Xu, H., Chen, J., Liu, Q., Deng, Y., Zeng, H., 2014. ACS Appl. Mater. Interfaces 6, 8845-8852.

Xie, Y., Lin, X.Y., Huang, Y.S., Pan, R.J., Zhu, Z., Zhou, L.J., Yang, C.J., 2015. Chem. Commun. 51, 2156-2158.

Xuan, F., Luo, X., Hsing, I.M., 2012. Anal. Chem. 84, 5216-5220.

Xuan, F., Hsing, I.M., 2014. J. Am. Chem. Soc. 136, 9810-9813.

Yang, L., Liu, C., Ren, W., Li, Z., 2012. ACS Appl. Mater. Interfaces 4, 6450-6453.

Zhuang, J., Lai, W., Chen, G., Tang, D., 2014. Chem. Commun. 50, 2935-2938.

Zhu, C., Zeng, Z., Li, H., Li, F., Fan, C., Zhang, H., 2013. J. Am. Chem. Soc. 135, 5998-6001.

Zhu, W.Y., Su, X.P., Gao, X.Y., Dai, Z., Zou, X.Y., 2014. Biosens. Bioelectron. 53, 414-419.

Figure captions:

Fig. 1. (A) SEM image of Fe_3O_4@PDA NPs. (B) TEM image of Fe_3O_4@PDA NPs. The inset is a higher magnification image of the polydopamine shell layer of Fe_3O_4@PDA core-shell nanoparticles.

Scheme 1. Diagram illustration for sensitive detection of target DNA based on core-shell Fe_3O_4 polydopamine nanoparticles and hybridization chain reaction amplification.

Fig. 2. (A) Fluorescence emission spectra of different samples (curves a-c). a: H1, H2; b: H1, H2, Fe_3O_4@PDA NPs; c: target DNA, H1, H2, Fe_3O_4@PDA NPs. Concentrations: Fe_3O_4@PDA NPs (1.8 mg mL^{-1}), H1 (1.0×10^{-7} mol L^{-1}), H2 (1.0×10^{-7} mol L^{-1}), and target DNA (7.0×10^{-9} mol L^{-1}). (B) Effects of different concentrations of Fe_3O_4@PDA NPs on fluorescence signal decrease percentage of hairpins with different lengths of sticky ends. Concentrations: Fe_3O_4@PDA NPs (1.2, 1.8, and 2.4 mg mL^{-1}), HP0 (2.0×10^{-7} mol L^{-1}), HP6 (2.0×10^{-7} mol L^{-1}), HP12 (2.0×10^{-7} mol L^{-1}), and HP18 (2.0×10^{-7} mol L^{-1}).

Fig. 3. Fluorescence emission spectra with the addition of different concentrations of target DNA (curves a-l). Inset: Linear relationship between the fluorescence intensity and the concentration of target DNA. Concentrations: Fe_3O_4@PDA NPs (1.8 mg mL^{-1}), H1 (1.0×10^{-7} mol L^{-1}), H2 (1.0×10^{-7} mol L^{-1}), and target DNA (a-l: 0, 0.1, 0.2, 0.3, 0.4, 0.5, 0.7, 1.0, 1.5, 2.0, 5.0, and 7.0 nM).

Fig. 4. Specificity evaluation of the sensing method for target DNA against mismatched DNA sequences. T, M1, D1, and M3 represent the perfectly complementary sequence, one base-mismatched sequence, one base-deleted sequence, and three-base mismatched sequence. Concentrations of target DNA and other mismatched DNA were all 0.5 nM. Concentrations: Fe_3O_4@PDA NPs (1.8 mg mL^{-1}), H1 (1.0×10^{-7} mol L^{-1}), and H2 (1.0×10^{-7} mol L^{-1}).

Fig. 1.

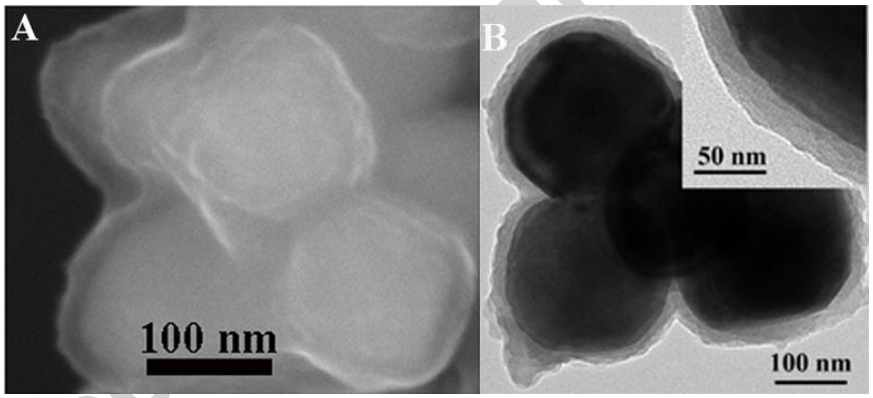

Scheme 1.

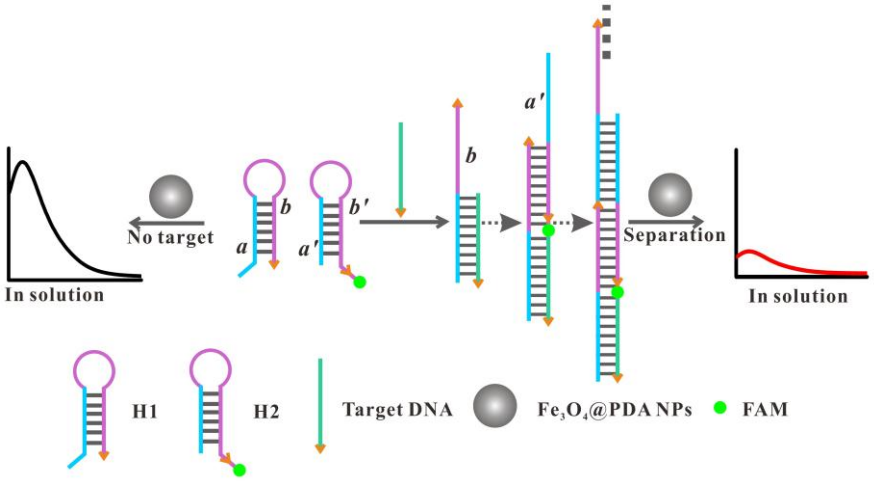

Fig. 2.

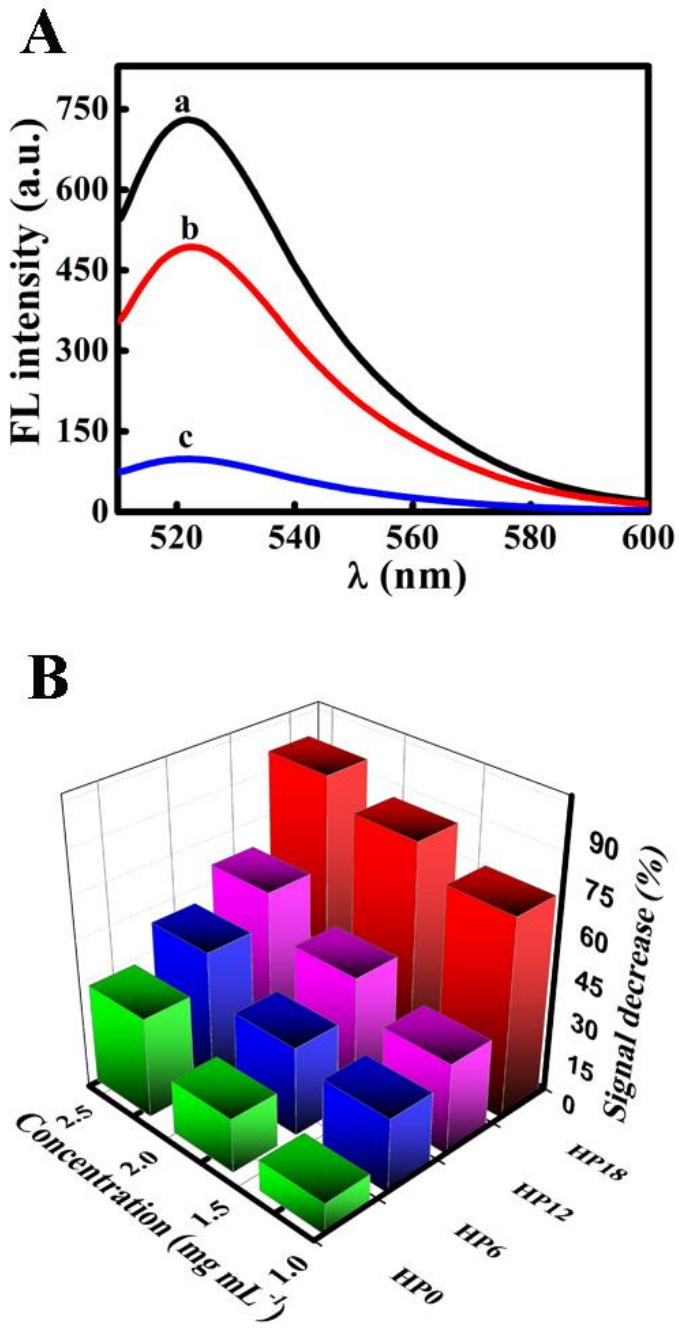
A
FL intensity (a.u.)
750
600
450
300
150
0
a
b
c
520
540
560
580
600
λ (nm)
B
Signal decrease (%)
90
75
60
45
30
15
0
HP18
HP12
HP6
HP0
Concentration (mg mL-1)

Fig. 3.

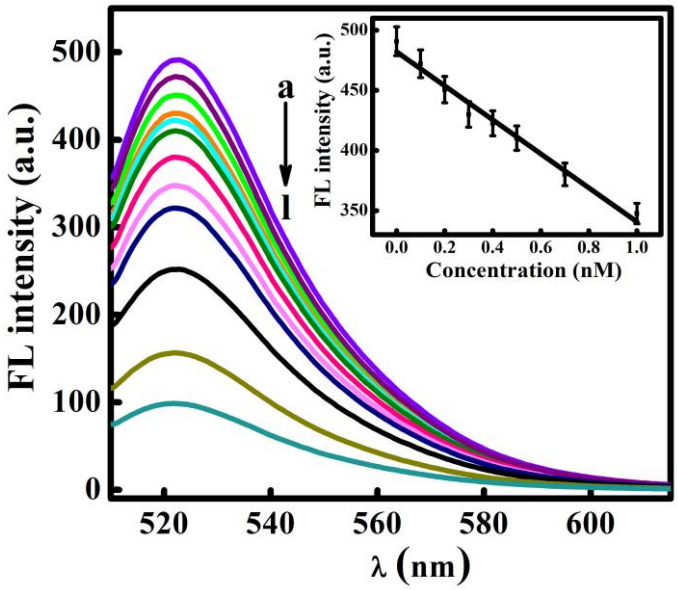

Fig. 4.

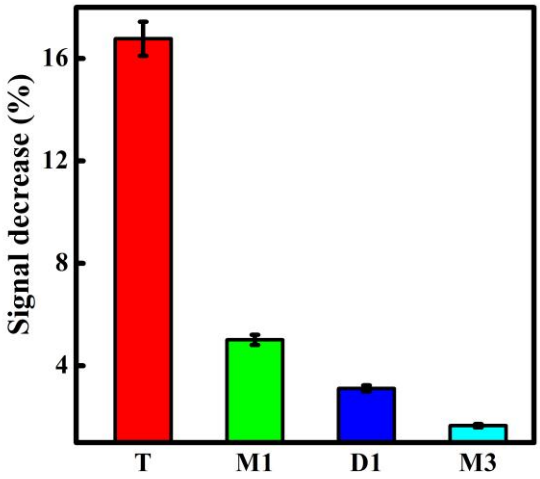

For TOC only

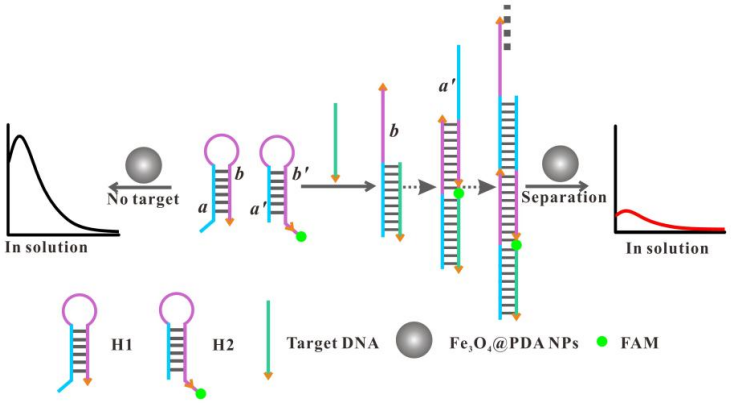

Highlights

► Enzyme-free DNA detection was developed based on HCR and Fe_3O_4@PDA NPs.

► Signal amplification was achieved by hybridization chain reaction.

► Fe_3O_4@PDA NPs were used for homogeneous and rapid HCR products capture efficiently.

► The strategy could distinguish single-base mismatched DNA sequence.